A Novel Approach to Determine Static Voltage Stability Limit and Its Improvement Using TCSC and SVC

C. K. Babulal*, P. S. Kannan* and J. Maryanita**
**Dept. of Electrical and Electronics Engg., Thiagarajar College of Engg., Madurai, India*
***Dept. of Electrical and Electronics Engg., National College of Engg., Tirunelveli, India*
Email: ck_babulal@yahoo.co.in
(Received on 16 Mar 2005, revised on 1 Oct 2005)

Abstract

Determination of the steady state voltage stability is essential in power system operation and planning. Conventional method of finding the maximum or critical loading point (CLP), suffers from huge computational time and iteration. In this paper an adaptive neuro fuzzy inference system (ANFIS) is used to control the step length of a conventional continuation power flow (CPF) method in determining CLP and nose curves (PV – curves). Modal analysis technique is adopted to identify the vulnerable load buses and critical branches of a power system, for the effective placement of FACTS devices. Static VAR Compensator (SVC) and Thyristor Controlled Series Capacitor (TCSC) are used in the identified location to enhance the static voltage stability limit of the power system. The proposed approach is successfully applied to 9 bus, New England 39 bus and IEEE 118 bus system and the results are reported.

Introduction

Determination of the steady state voltage stability is essential in power system operation and planning. Deregulated policies, environment legislation, construction cost of new transmission lines, continuous growth in demand are main factors forcing the utilities to operate their system closer to maximum power transfer capability limits. Consequently, the risk of voltage instability or voltage collapse increases. It is evident from various voltage collapse incidents occurred around the world [1-3]. Thus, the determination of voltage stability limit at various operating condition is essential to operate the system with sufficient safety margin.

The main factor causing instability is the inability of the power system to meet the demand for reactive power. In general, two approaches are available to assess the voltage stability viz., static and dynamic. Static voltage stability analysis is based on the solution of conventional or modified power flow equations. It provides the ability of transmission network to support a specified load demand. On the other hand, the dynamic approach tries to find why and how the voltage collapse has occurred.

Several methods are already proposed in the literature to determine the static stability limit like the P-V and Q-V curves, multiple load flow solution, Continuation Power Flow (CPF), minimum Eigen value, sensitivity, and energy based method, and bifurcation theory methods [1, 4-11]. Recently, researchers have tried a fast method suitable for on-line applications [12-14]. All the methods involve heavy computational steps and time, because it depends on the choice of step length control.

System modeling based on the conventional mathematical tools is not well suited for dealing with ill-defined and uncertain systems. In contrast, a Fuzzy Inference System can model the qualitative aspects of

human knowledge and reasoning process without employing precise quantitative analysis [15]. The Fuzzy modeling has been found numerous practical applications in various fields. It is also effectively used in power systems [16-19].

In this paper, a new approach is proposed using Adaptive Neuron Fuzzy Inference System (ANFIS). The selection of step length during the trace of Nose curve is effectively done by ANFIS step length controller, from the magnitude of bus voltage and change in bus voltage. ANFIS in MATLAB software package is used for generation of membership functions and control rules, of a step length controller.

Flexible AC Transmission System (FACTS) devices are being increasingly utilized in many electric power systems to enhance voltage control and system dynamic performance. FACTS devices can enable the transmission line to carry power closer to their thermal limits, while maintaining and/or improving network security or reliability. Among the available FACTS devices SVC and TCSC are widely used for improving steady state voltage stability [20-21]. For the placement of FACTS devices, it is essential to identify the vulnerable buses and branches of a power system. To identify it, there are number of algorithms have been proposed in the literature. Among them, Modal Analysis of the reduced Jacobian matrix has been widely used as a static voltage stability index [22]. This analysis is used in the paper find the vulnerable load buses and critical branches, for the effective placement of FACTS devices.

The proposed approach is effectively used for 9 bus [23], 39 bus [4] and IEEE 118 bus test systems for various loading scenarios and the results shows that the FACTS devices improve the steady state voltage stability significantly. The organization of the paper is as follows. Following the introduction, some preliminary background on ANFIS is provided in Section II. In Section III, the design of ANFIS step length controller is given. In Section IV, stability enhancement using FACTS devices are provided. In Section V, algorithm of the proposed approach is given. In Section VI, computer simulation is performed to prove the effectiveness of the suggested method. Finally, some conclusions are drawn in Section VII.

Adaptive Neuron Fuzzy Inference System (ANFIS)

The design objective of the fuzzy controller is to learn and achieve good performance in the presence of disturbances and uncertainties. The design of membership functions is done by the ANFIS batch learning technique, which amounts to tune a FIS with back propagation algorithm based on a collection of input – output data pairs.

ANFIS architecture

Generally, ANFIS is a multilayer feed forward network in which each node performs a particular function (node function) on incoming signals. For simplicity, we consider two inputs ‘x’ and ‘y’ and one output ‘z’. Suppose that the rule base contains two fuzzy if-then rules of Takagi and Sugeno type [15].

$$\begin{aligned} &\text{Rule 1: IF } x \text{ is } A_1 \text{ and } y \text{ is } B_1 \text{ THEN } f_1 = P_1 x + Q_1 y + R_1 \\ &\text{Rule 2: IF } x \text{ is } A_2 \text{ and } y \text{ is } B_2 \text{ THEN } f_2 = P_2 x + Q_2 y + R_2 \end{aligned} \quad (1)$$

The ANFIS architecture shown in Fig. 1 is a five layer feed forward network as follows.

Layer 1: Every node in this layer is a square node with a node function (the member ship value of the premise part)

$$O_i^1 = \mu_{Ai}(x) \tag{2}$$

where, x is the input to the node i, and A_i is the linguistic label associated with this node function.

Layer 2: Every node in this layer is a circle node labeled Π which multiplies the incoming signals. Each node output represents the firing strength of a rule.

$$O_i^2 = \mu_{Ai}(x)\,\mu_{Bi}(y) \text{ where, i = 1:2} \tag{3}$$

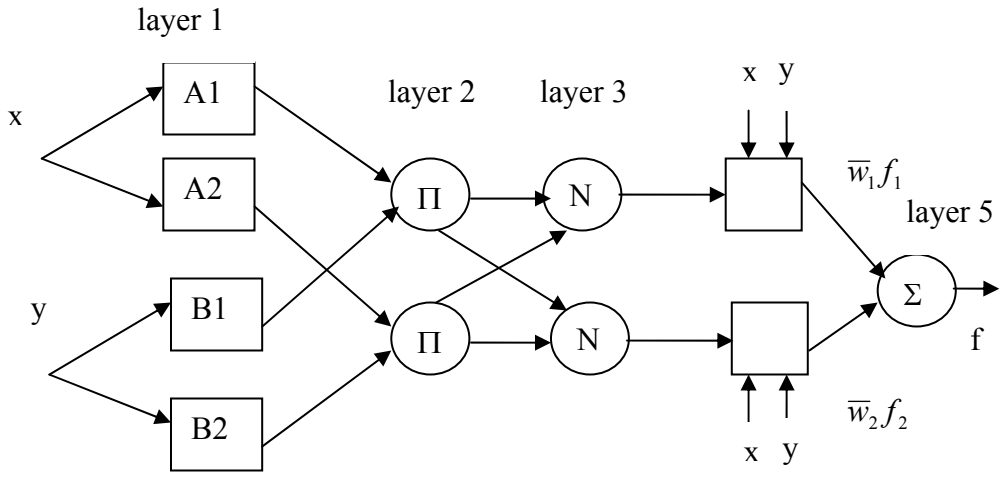

Fig. 1 The ANFIS architecture

Layer 3: Every node in this layer is a circle node labeled N (normalization). The i^{th} node calculates the ratio of the i^{th} rule's firing strength to the sum of all firing strengths.

$$O_i^3 = \overline{W_i} = \frac{W_i}{W_1 + W_2} \text{ , where, i=1: 2} \tag{4}$$

Layer 4: Every node in this layer is a square node with a node function

$$O_i^4 = \overline{W_i} f_i = \overline{W_i}(P_i x + Q_i y + R_i) \text{ , where i=1:2} \tag{5}$$

Layer 5: The single node in this layer is a circle node labeled Σ that computes the overall output as the summation of all incoming signals

$$O_i^5 = \text{System output, where i = 1:2} \tag{6}$$

"Eq. (6)" represents the overall output of the ANFIS, which is functionally equivalent to the fuzzy system in "Eq. (1)"

ANFIS learning algorithm

In this subsection the hybrid learning algorithm is explained briefly. The hybrid learning algorithm is a combination of both the back propagation and the least square algorithms. The back propagation is used to identify the nonlinear parameters (premise parameters) and the least square is used for the linear parameters in the consequent parts.

From the ANFIS structure given above, it has been observed that when the values of the premise parameters are fixed, the overall output can be expressed as a linear combination of the consequent parameters. That is the output in layer 5 "Eq. (6)" can be rewritten as

$$f = \frac{W_1}{W_1 + W_2} f_1 + \frac{W_2}{W_1 + W_2} f_2$$

$$f = \overline{W_1} f_1 + \overline{W_2} f_2$$

$$f = \overline{W_1}(P_1 x + Q_1 y + R_1) + \overline{W_2}(P_2 x + Q_2 y + R_2)$$

$$f = (\overline{W_1} x)P_1 + (\overline{W_1} y)Q_1 + (\overline{W_1})R_1 + (\overline{W_2} x)P_2 + (\overline{W_2} y)Q_2 + (\overline{W_2})R_2 \quad (7)$$

This is linear in the consequent parameters P1, Q1, R1, P2, Q2, and R2.

From this observation, the whole system parameter set can be represented as S= [S1 S2] where S1 is the set of nonlinear parameters and S2 is the set of linear parameters. The hybrid learning algorithm is a combination of both back propagation and the least square algorithms. Each epoch of the hybrid learning algorithm consists of two passes, namely forward pass and backward pass. In the forward pass of the hybrid learning algorithm, functional signals go forward up to layer 4 and the consequent parameters are identified by the least squares estimate.

In the backward pass the error rates propagates in the backward direction and the premise parameters are updated by the gradient descent method. The two pass procedure in the hybrid-learning algorithm for ANFIS are summarized in Table 1 [15].

Table 1 Two pass procedure in the hybrid-learning algorithm for ANFIS

	Forward	**Backward**
Premise Parameters	Fixed	Gradient Descent
Consequent Parameter	Least square Estimation(LSE)	Fixed
Signals	Node Outputs	Error Rates

ANFIS Step Length Controller

The functional block diagram of the ANFIS step length controller is shown in Fig. 2. Where x and Δx are load bus voltage and change in load bus voltage in p.u. Δt is the incremental loading parameter.

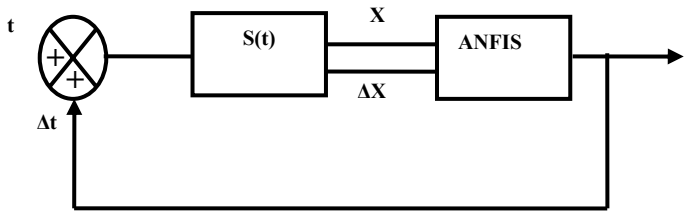

Fig. 2 Functional block diagram of ANFIS step length controller

The ANFIS step length control has two inputs, the bus voltage and change in bus voltage, and one output step length. Fig. 3 shows the architecture of the ANFIS step length controller.

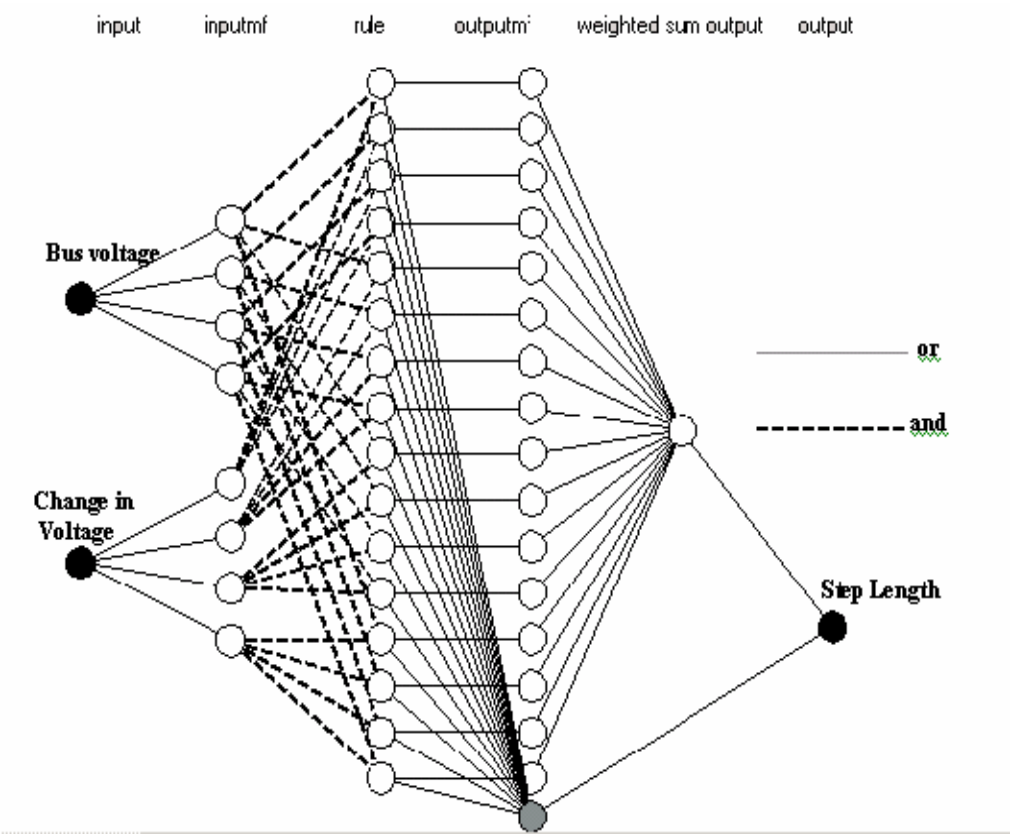

Fig. 3 Architecture of ANFIS step length controller

The design steps are as follows:

- The computational efficiency of any continuation power flow method is depends on the choice of effective step length control [7]. Ideally the step length should be selected according to the shape of the nose curve to be traced, and it is unknown beforehand. Thus, making the task of designing the effective step length control difficult. From the nose curve of Fig. 4, one can observe that when the system is operating near the base case, the decrease in bus voltage due to an increase in load is less. In contrast, decrease in voltage will be large when the system is operating near the critical loading. This leads to an idea of choosing larger step length at lightly loaded conditions and smaller step length at stressed condition.

- The performance of ANFIS controller is depends on the size of the training data set. Thus the training data for the step length controller should cover the wide range of all possibilities of bus voltages and change in bus voltages.

- The training data for the ANFIS step length controller is selected from the Homotophy continuation method [4- 5].

- This training data yields the membership functions, which are shown in Fig. 5.

- ANFIS is trained using 100 epochs and an initial step size of 10-4 which was the best step found that gives acceptable error convergence.

- The number of membership functions, their range and the amount of overlapping are changed in order to fit the training data output.

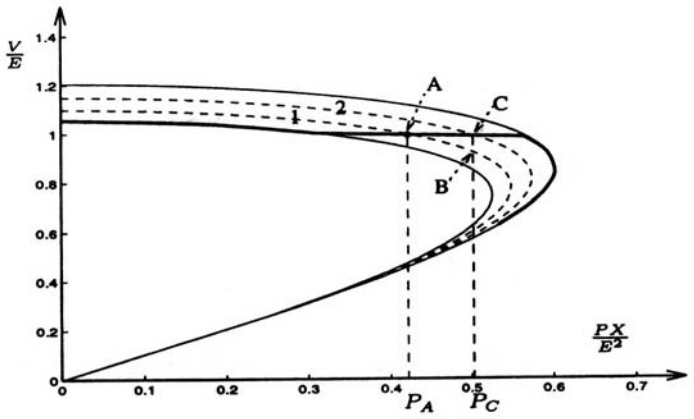

Fig. 4 Nose curves reflecting the effects of SVC

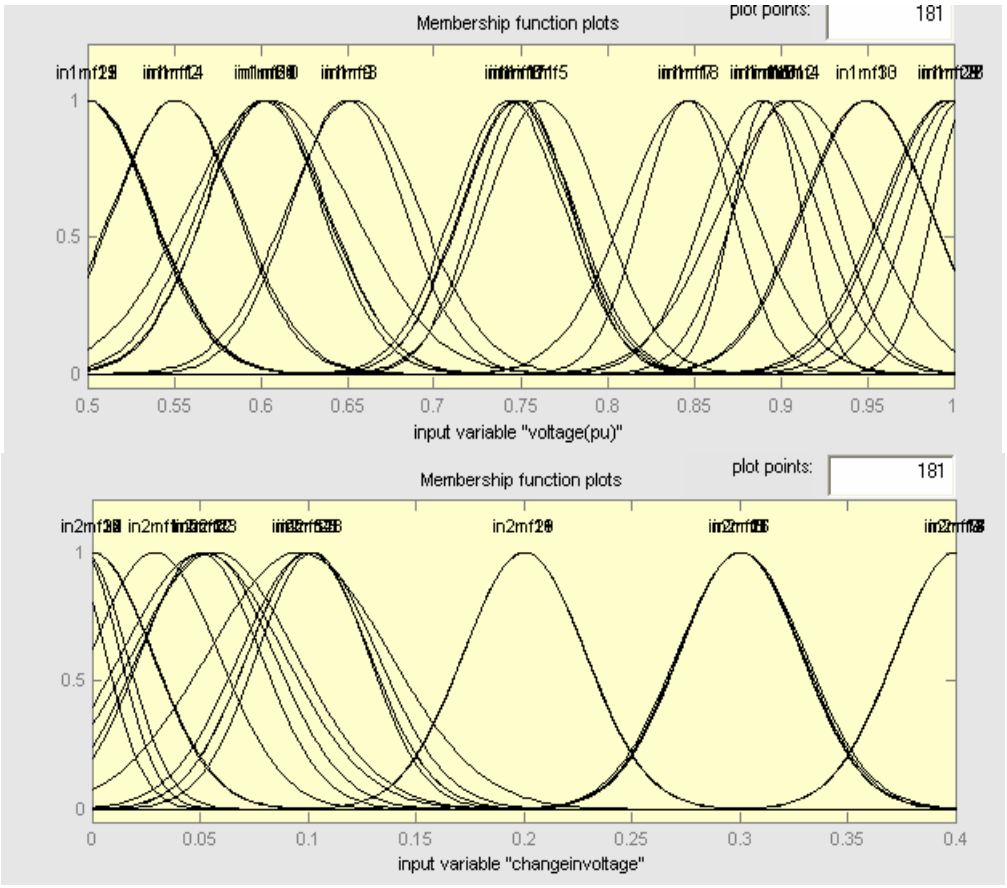

Fig. 5 Membership function of input variables

Stability Enhancement Using Facts Devices

Static VAR compensator

The most popular configuration of shunt devices are the fixed capacitor and the thyristor controlled reactor (FC-TCR) and the thyristor switched capacitor, thyristor controlled reactor (TSC-TCR) from steady state perspective. In this paper, the fixed capacitor model is adapted and the block diagram of the SVC is shown in Fig. 6.

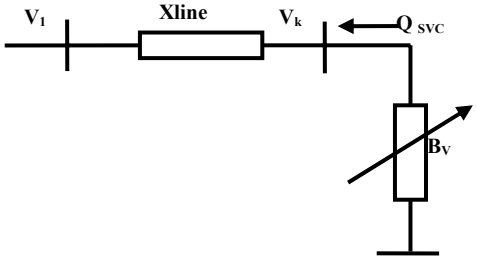

Fig. 6 Block diagram of SVC

Assume for instance that the system is operating initially at point 'A' on the dashed nose curve numbered 1 and that the load power is increased from PA to PC. In the absence of SVC action the new operating point would be 'B'. However this causes a voltage drop that the SVC will counteract by increasing its VAR injection [13].

The operating point will shift to curve 2 and new operating point is 'C'. All operating points will fall on the lightly sloping line which corresponds to voltage control by SVC.

SVC is a shunt compensation component. When it is installed in the transmission line, it can be treated as a PV bus with the generation of real power as zero.

Thyristor controlled series capacitors

Series capacitive compensation can also be used to reduce the series reactive impedance to minimize the receiving end voltage variation and the possibility of voltage collapse. The placement of series capacitor at the critical branch will move the critical loading point to a higher value. Series capacitive compensation effectively increases the voltage stability limit by canceling a portion of the line reactance and thereby, in effect, providing a "stiff" voltage source for the load. Fig. 7 shows the block diagram of the TCSC, and Fig. 8 sketches the Nose curves for various levels of compensation.

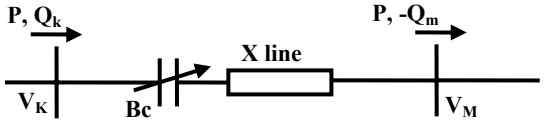

Fig. 7 Block diagram of TCSC

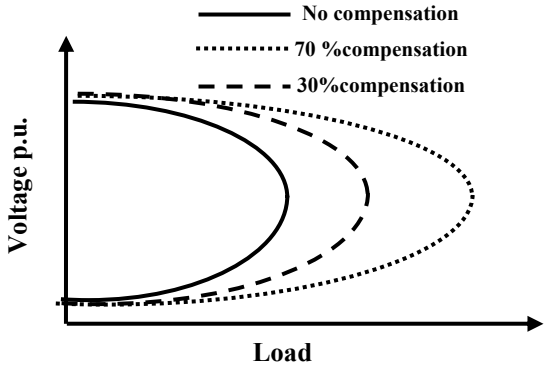

Fig. 8 Nose curves for various levels of compensation

The Homotophy Continuation Method (HCM) is documented in [5]. In HCM, the critical loading condition and nose curves are obtained by solving the Homotophy function (1):

$$H(x, t) = Y(x) - Ys(t) \quad (8)$$

$$Ys(t) = Yso + t * Yd \quad (9)$$

where, Yso - specified value of base load in p.u.
Yd - loading/generating pattern
t - Homotophy scalar parameter
Ys(t) - loading pattern linear above the base load
x - voltage vector in p.u.

The solution of H(x, t) = 0, provides a load flow solution for specified value of *Ys(t)*. The loading /generating pattern varies according to the chosen scenario.

Algorithm of the Proposed Approach

The algorithm for the determination of static voltage stability limit using ANFIS step length controller and its improvement using the FACTS devices are given in the following steps.

- Starting from the base condition the loads are increased in steps according to the "Eq.(9)"
- Using the ANFIS step length controller the step length of each continuation step is determined.
- Step 1 and 2 are repeatedly used till the error between the successive iteration of the ANFIS step length controller is less than the specified value.
- The bus voltage (V) and loading parameter (t) obtained in each iteration are plotted to obtain the nose curve. The value of P and Q at the convergence is the CLP.
- Using the idea of Modal analysis method [22], the set of critical singular values and associated right and left Eigen vectors of the reduced Jacobian matrix are calculated. The reduced Jacobian matrix (J_R) is defined as

$$J_R = \left[J_{QV} - J_{Q\theta} J_{P\theta}^{-1} J_{PV} \right] \quad (10)$$

$$J_R = \varepsilon \lambda \eta \quad 11)$$

where, ε - right eigen vector of J_R, η - left eigen vector J_R, λ - diagonal eigen value matrix of J_R

- For each voltage instability mode, the bus and branch participation is computed by using the "Eq. (11)" and (12) respectively.

$$P_{ki} = \varepsilon_{ki} \eta_{ki} \quad (12)$$

$$P_{lji} = \frac{\Delta Q_{lji}}{\Delta Q_{lj\ \max\ i}} \quad 13)$$

where, P_{ki} - participation factor of bus k to mode i , P_{lji} - participation factor of branch lj to mode i , ΔQ_{lji} - reactive power flow variation of branch lj , $\Delta Q_{lj\ max\ i}$ - maximum allowable reactive power flow variation of branch lj.

- The maximum entries in the participation vectors are the effective location of placing FACTS devices.
- SVC and TCSC are placed in the above identified location. Steps 1 - 4 are repeated to find the improvement in steady state voltage stability.

Case Study

To illustrate the ANFIS approach in determining the CLP and voltage stability enhancement using FACTS devices, 9 bus, New England 39 bus and IEEE 118 bus systems are considered. Two scenarios are adapted for all the systems. In scenario A, the real and reactive load at all load buses are increased simultaneously. Whereas in scenario B, the reactive power at any one of the load bus alone is increased. For both scenarios the loading pattern S_d is chosen as 10% of the initial loading condition. The nose curve of the system is investigated with and without FACTS devices under loading scenario A and scenario B.

SVC of 20MVAR, 300MVAR and 400MVAR are connected to the vulnerable buses selected from the modal analysis for 9 bus, 39 bus and 118 bus system respectively. The TCSC with 70% of the line reactance is connected to the critical branches obtained from the branch participation vector of Modal analysis.

The 9 bus system

Table 2 shows the bus data of the 9 bus system. The load and generation details with reactive power limits at the base case are given in the Table 2.

Table 2 The 9 bus system data

Bus No.	Voltage (p.u.)	Angle (deg.)	Load		Generation		Q_{limits} MVAR	
			MW	MVar	MW	MVar	Q_{min}	Q_{max}
1	1.040	0.000	0	0	0	0	0	0
2	1.025	0.000	0	0	163	0	-15	10
3	1.025	0.000	0	0	85	0	-15	10
4	1.000	0.000	0	0	0	0	0	0
5	1.000	0.000	60	90	0	0	0	0
6	1.000	0.000	90	60	0	0	0	0
7	1.000	0.000	0	0	0	0	0	0
8	1.000	0.000	105	65	0	0	0	0
9	1.000	0.000	0	0	0	0	0	0

Scenario A

In this scenario, the real and reactive powers at all load buses are increased uniformly. In a deregulated environment power transfer can occur in practice from any point of generation to any point of load. Table 3 shows a case study in which the increase in demand is supplied by the generator connected at the slack bus alone. Other case studies like, two generators or three generators and several possible combinations of supplying power to the load point were studied but not reported.

Table 3 The results of 9 bus system for various iterations in scenario A without FACTS devices

It. No	Generation				Load						t
	P_1 MW	Q_1 MVar	Q_2 MVar	Q_3 MVar	P_5 MW	Q_5 MVar	P_6 MW	Q_6 MVar	P_8 MW	Q_8 MVar	
0	12.20	73.90	41.19	21.22	60.00	90.00	90.00	60.00	105.00	65.00	0
2	69.19	86.89	46.47	33.43	82.59	99.04	106.26	65.42	123.07	71.32	1.807
4	126.61	115.93	47.97	49.45	104.99	107.99	122.39	70.80	140.99	77.60	3.599
6	149.85	150.56	49.75	48.87	113.80	111.52	128.73	72.91	148.04	80.06	4.304
8	164.17	193.82	46.72	49.91	118.87	113.55	132.39	74.13	152.09	81.48	4.709
10	175.45	220.39	49.04	49.91	122.87	115.15	135.27	75.09	155.30	82.60	5.819

Table 3 shows scenario A results of the 9 bus system without FACTS devices for some of the iteration. The details of load increase at bus 5, 6 and 8 and the corresponding increase in the generation and the value of continuation parameter 't' obtained from the ANFIS controller are given in the Table 3. The convergence (the difference between the two successive values of 't' is less than the specified error value) takes place at the 10^{th} iteration, at which the value of t= 5.8194 and the corresponding CLP is 413.432 MW, 272.84 MVar.

Using the Modal analysis method, the bus and branch participation vectors are calculated and are shown in Fig. 9.

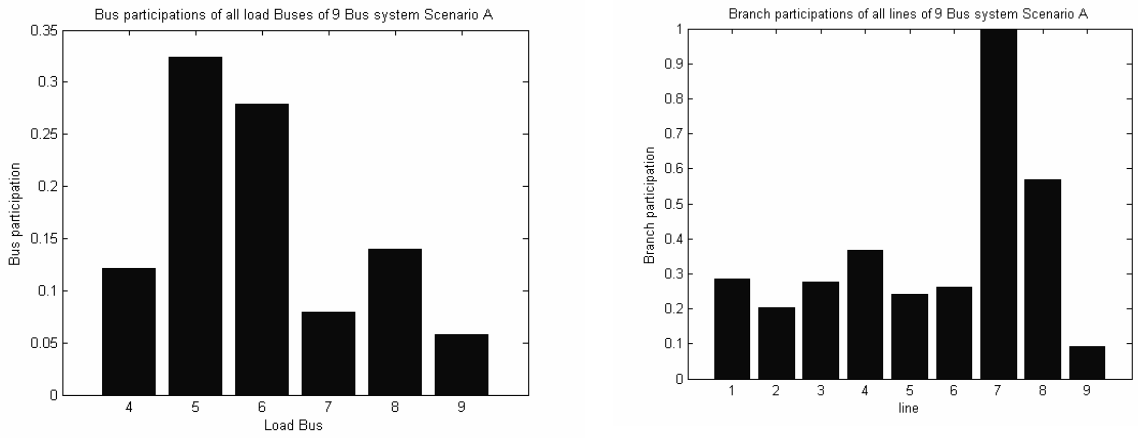

Fig. 9 Bus and Branch Participation Vectors of the 9 bus Scenario A

The highest values of participation vector are the candidate for the location of FACTS devices. In this case a SVC of 20 MVar is connected at the bus 5. The procedure for determination of CLP is repeated and the new value of CLP is calculated as 440.961 MW, 282.891 MVar. Thus an increase in loading of 27.527 MW, 10.051 MVar is obtained due to the inclusion of SVC. Similarly TCSC (70% of the line reactance of the critical line) is connected between the bus 4 -1, and the new CLP is 550.773 MW, 322.98 MVar and the

improvement in the loadings is 137.341 MW, 50.14 MVar. Fig. 10 shows the nose curve of the 9 bus system with and without FACTS devices.

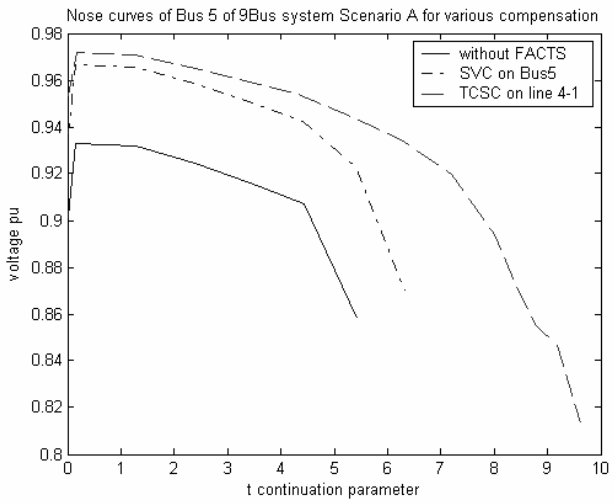

Fig. 10 Nose curves for various levels of compensation for 9 bus scenario A

Table 4 shows the CLP (first entry is P in MW and the second entry is Q in MVar) and its corresponding loading parameter obtained at the voltage collapse point of all test system with and without FACTS devices. It is clear that the placement of TCSC gives better performance except in 39 bus system in scenario B.

Table 4 Comparison of CLP in the studied system with and without FACTS devices

	Test System	Without FACTS device		With SVC		With TCSC	
		CLP(P,Q)	t	CLP(P,Q)	T	CLP(P,Q)	t
Scenario A	9 Bus system	413.432 272.840	5.8194	440.961 282.891	7.0218	550.773 322.980	9.739
	39 Bus system	8568.945 2094.151	4.6738	8695.915 2125.480	4.9234	8779.749 2146.167	5.088
	118 Bus system	5997.995 2300.760	7.8921	6163.1 2363.1	8.2287	6190.5 2373.4	8.319
Scenario B	9 Bus system	255.00 595.07	17.6775	255.00 671.24	21.220	255.00 1008.7	36.91
	39 Bus system	6097.100 2995.779	21.7376	6097.100 3294.035	27.702	6097.100 3149.052	24.80
	118 Bus system	3678.00 1740.0	2.7632	3678.00 2143.9	6.3060	3678.00 2309.50	7.758

Scenario B

The CLP is determined without FACTS devices and it is found as t=17.6775 .The bus and branch participation vectors are calculated and shown in Fig. 11. The bus 5 and the line 4 -1 are selected for placement of SVC and TCSC respectively. The CLP is determined using ANFIS controller and the Fig. 12 shows the improvement in voltage profile and in CLP. With SVC the CLP is calculated as t=21.2203, and with TCSC it is determined as t=36.9171.

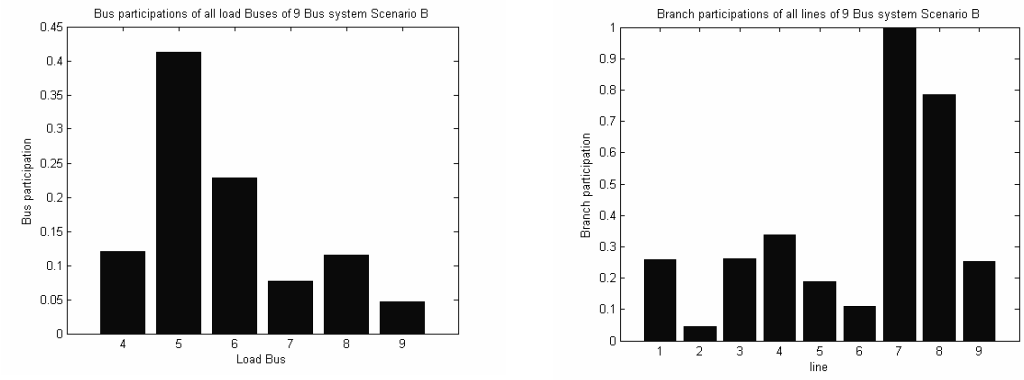

Fig. 11 Bus and branch participation vectors of 9 bus scenario B

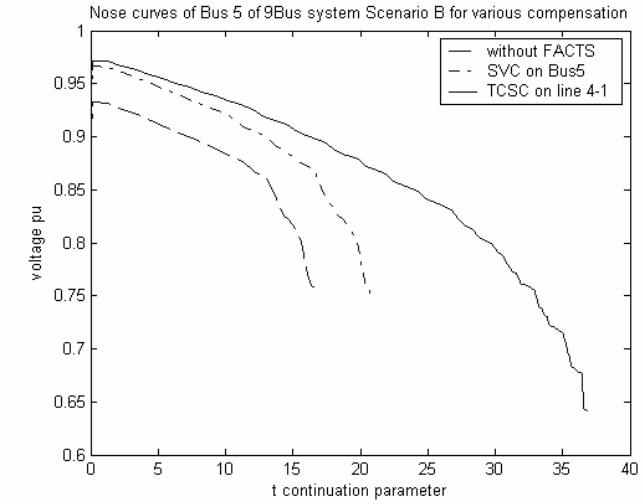

Fig. 12 Nose curves for various levels of compensation for 9 bus scenario B

The 39 bus new England system

Scenario A

The CLP is determined without FACTS devices and it is found as t=4.5915 .The bus and branch participation vectors are calculated and shown in Fig. 13. The bus 8 and the line 9-39 are selected for placement of SVC and TCSC respectively. The CLP is determined using ANFIS controller and the Fig. 14

shows the improvement in voltage profile and in CLP. With SVC the CLP is calculated as t=4.9128, and with TCSC it is determined as t=5.0716.

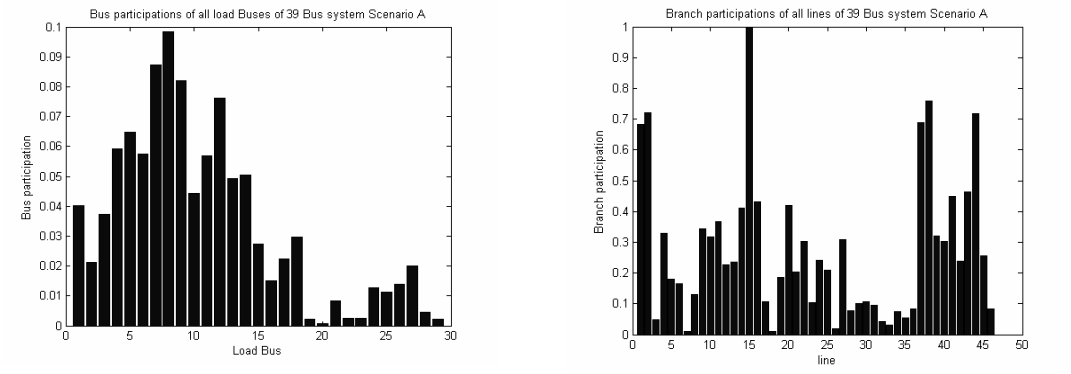

Fig. 13 Bus and branch participation vectors of 39 bus scenario A

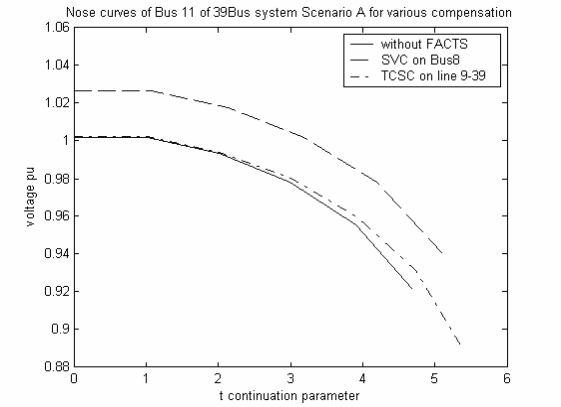

Fig. 14 Nose curves for various levels of compensation for 39 bus scenario A

Scenario B

The CLP is determined without FACTS devices and it is found as t=21.6751. The bus and branch participation vectors are calculated and shown in Fig. 15. The bus 11 and the line 10-32 are selected for placement of SVC and TCSC respectively. The CLP is determined using ANFIS controller and the Fig. 16 shows the improvement in voltage profile and in CLP. With SVC the CLP is calculated as t=27.7154, and with TCSC it is determined as t=24.6839.

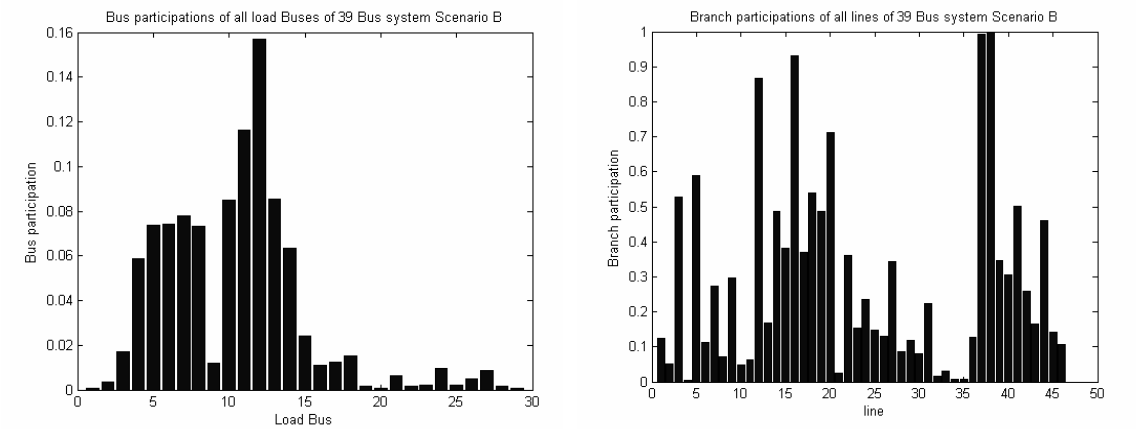

Fig. 15 Bus and branch participation vectors of 39 bus scenario B

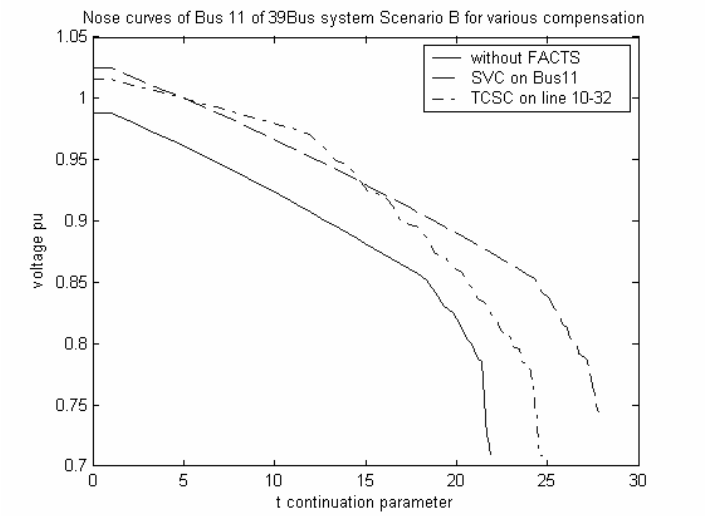

Fig. 16 Nose curves for various levels of compensation for 39 bus scenario B

The IEEE 118 bus system

Scenario A

The CLP is determined without FACTS devices and it is found as t=7.8921 .The bus and branch participation vectors are calculated and shown in Fig. 17. The bus 75 and the line 69-90 are selected for placement of SVC and TCSC respectively. The CLP is determined using ANFIS controller and the Fig. 18 shows the improvement in voltage profile and in CLP. With SVC the CLP is calculated as t=8.2287, and with TCSC it is determined as t= 8.3195.

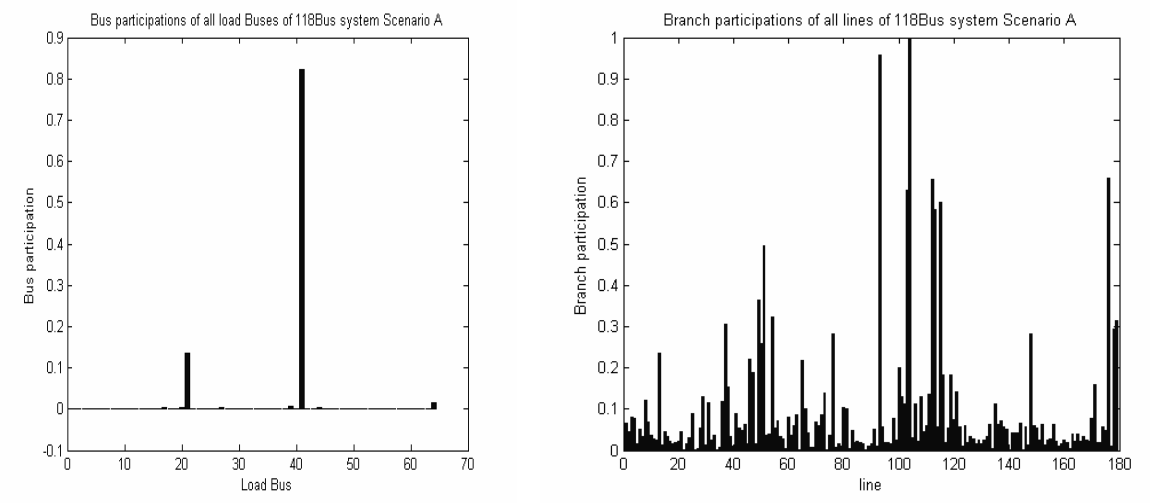

Fig. 17 Bus and branch participation vectors of 118 bus scenario A

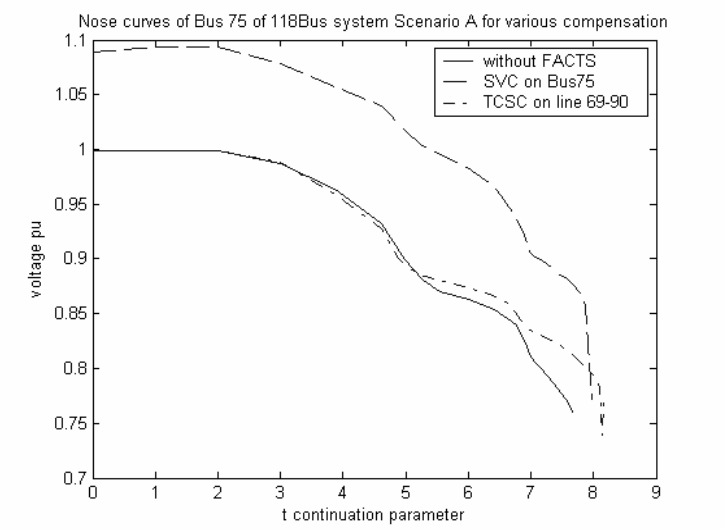

Fig. 18 Nose curves for various levels of compensation for 118 bus scenario A

Scenario B

The CLP is determined without FACTS devices and it is found as t=2.7632.The bus and branch participation vectors are calculated and shown in Fig. 19. The bus 67 and the line 66-67 are selected for placement of SVC and TCSC respectively. The CLP is determined using ANFIS controller and the Fig. 20 shows the improvement in voltage profile and in CLP. With SVC the CLP is calculated as t=6.3060, and with TCSC it is determined as t=7.7588.

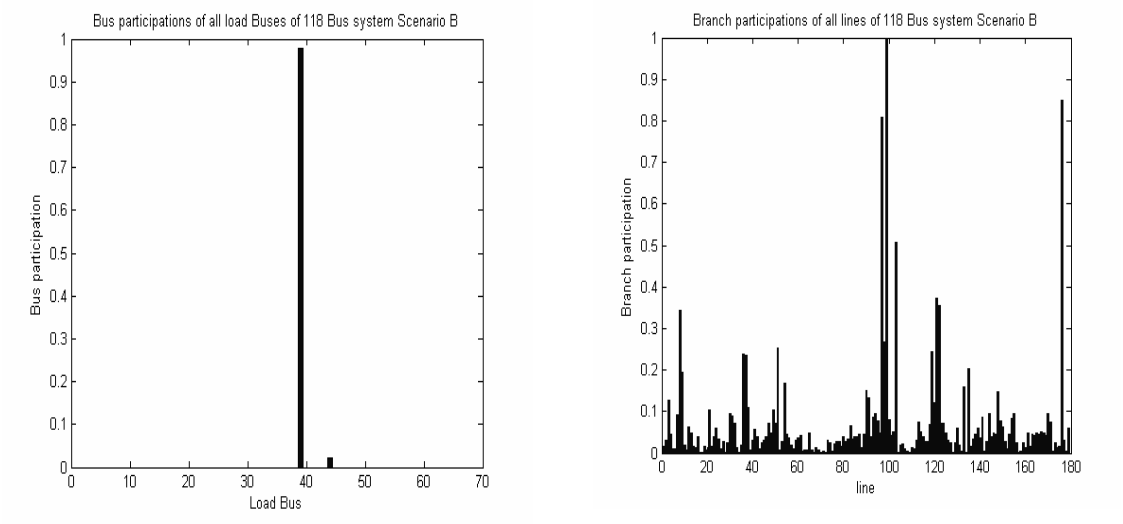

Fig. 19 Bus and branch participation vectors of 118 bus scenario B

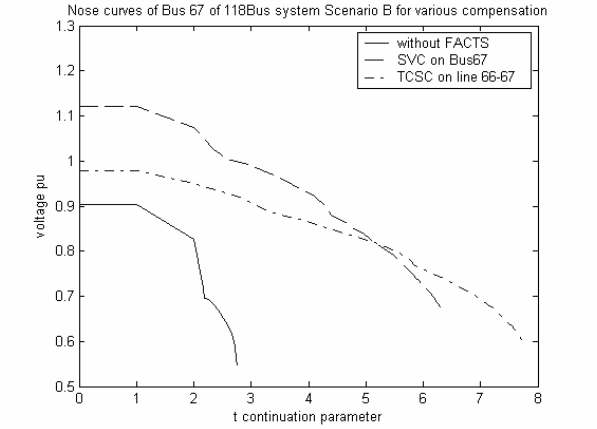

Fig. 20 Nose curves for various levels of compensation for 118 bus scenario B

Conclusion

In this paper, an ANFIS step length controller design is proposed and an attempt is made to increase the loadability limit of the 9 bus, New England 39 bus, and IEEE 118 bus test systems with SVC and TCSC. Eigen vector analysis combined with continuation power flow and FACTS, provided promising results for the test systems taken. Other studies show that the uncoordinated application of multiple FACTS devices can actually decrease the steady state voltage stability.

Acknowledgement

The authors wish to thank the Management, Principal, and Staff of Thiagarajar College of Engineering, Madurai for providing necessary facilities to carry out this work.

References

[1] C. W. Taylor, "Power system voltage stability," McGraw Hill, New York, 1994.

[2] P. Kundur, "Power system stability and control," The EPRI power engineering series, McGraw Hill, 1994.

[3] T. V. Cutsem and C. Vournas "Voltage stability of electric power systems," Kluwer Academic Publishers, 1998.

[4] Y. Tamura, K. Sakamoto and Y. Tayama, "Voltage instability proximity index (VIPI) based on multiple load flow solutions in ill-conditioned power systems," In Proc., 27th Conference on decision and control, Austin, Texas, USA, 1988, pp. 2114-2119.

[5] K. Iba, H. Suzuki, M. Egawa, and T. Watanabe, "A method for finding a pair of multiple load flow solutions in bulk power systems," IEEE trans. on power systems, Vol. 6, No. 2, 1991, pp. 584-593.

[6] V. Ajjarapu, and C. Christy, "The continuation power flow: A tool for steady state voltage stability analysis," IEEE trans. on power systems, Vol. 7, No. 1, 1992, pp. 416-423

[7] H. D. Chiang, A. J. Fluek, K. S. Shah, and N. Balu, "CPFLOW: A practical tool for tracing power system steady state stationary behavior due to load and generation variation," IEEE trans. on power systems, 10 (2) (1995) 623-633

[8] P. A. Loof, T. Smed, G. Andersson and D. J. Hill, "Fast calculation of a voltage stability index," IEEE trans. on power systems, Vol. 7, No. 1, 1992, pp. 54–60.

[9] M. M. Begovic and A. G. Phadke, "Control of voltage stability using sensitivity analysis," IEEE trans. on power systems, Vol. 7, No. 1, 1992, pp. 114-123.

[10] C. L. DeMarco and T. J. Overbye "Improved techniques for power system voltage stability assessment using energy methods," IEEE trans. on power systems, Vol. 6, No. 4, 1991, pp.1446-1452.

[11] C. A. Canizares, "On bifurcations, voltage collapse and load modeling," IEEE trans. power systems, Vol. 10, No. 1, 1995, pp.512–518.

[12] N. Yorino, H. Q. Li, S. Harada, A. Ohta and H. A. Sasaki, "Method of voltage stability evaluation for branch and generator outage contingencies," IEEE trans. power systems, Vol. 19, 2004, pp. 252–259.

[13] M. H. Haque, "On-line monitoring of maximum permissible loading of a power system within the voltage stability limits," In IEE Proc., Generation transmission distribution, Vol. 150, No. 1, 2003, pp. 107–112.

[14] G. Verbic and F. Gubina, "Fast voltage-collapse line-protection algorithm based on local phasors," In IEE Proc., Generation transmission distribution, Vol. 150, No. 4, 2003, pp. 482–486.

[15] J. R. Jang, "ANFIS: Adaptive network based fuzzy inference system," IEEE trans. on power systems, Man and Cybernatics, Vol. 23, No. 3, 1993, pp.665 – 685.

[16] K. Euntai, "A new computational approach to stability analysis and synthesis of linguistic fuzzy control system," IEEE trans. on fuzzy systems, Vol. 12, No. 3, 2004, pp. 379 – 388.

[17] C. K. Babulal and P. S. Kannan, "Application of fuzzy logic to transient stability assessment," The 6th international power engineering conference (IPEC), Singapore, 2003, pp. 123 – 128.

[18] J. G. Vlachogiannis, "Fuzzy logic application in load flow studies," In IEE Proc., Generation transmission distribution, Vol. 148, No. 1, 2001, pp. 34-40.

[19] R. B. Cvhedid, S. H. Karki, Chadiel and Charmali, "Adaptive fuzzy control for wind diesel power system," IEEE transactions on energy conversion, Vol. 15, No. 1, 2000, pp. 71-78.

[20] M. Moghovemi and M. O. Faruque, "Effects of FACTS devices on static voltage stability," In Proc., TENCON, 2000, pp. 357- 362.

[21] M. A. Perez, A. R. Messina, C. R. Fuerte and Esquivel, "Application of FACTS devices to improve steady state voltage stability," In Proc., IEEE power engineering society summer meeting, 2000, pp. 1115 – 1120.

[22] B. Goa, G. K. Morison and P. Kundur, "Voltage stability evaluation using modal analysis, IEEE trans. on power systems, Vol. 7, No. 4, 1992, pp. 529 – 1541.

[23] P. M. Anderson and A. A. Faoud, "Power system control and stability," Galgotia publications, Indian English language edition, 1981.